



# Fusion of Brain Imaging Data with Artificial Intelligence to detect Autism Spectrum Disorder

Monalin Pal<sup>\*1</sup>, Rubini P. <sup>2</sup>

<sup>1</sup>CMR University (CMRU), Bangalore, India

<sup>2</sup>CMR University (CMRU), Bangalore, India

Emails: [monalin.19cphd@cmr.edu.in](mailto:monalin.19cphd@cmr.edu.in); [rubini.p@cmr.edu.in](mailto:rubini.p@cmr.edu.in)

## Abstract

Autism, a developmental and neurological disorder, impacts communication, interaction, and behavior, setting individuals with it apart from those without. This spectrum disorder affects various aspects of an individual's life, including social, cognitive, emotional, and physical health. Early detection and intervention are crucial for symptom reduction and facilitating learning and development. Recent advancements in machine learning and deep learning have facilitated the diagnosis of Autism by analyzing brain signals. This current study introduces an approach for Autism detection utilizing functional Magnetic Resonance Imaging (fMRI) data. The Autism Brain Imaging Data Exchange (ABIDE) dataset serves as the foundation, employing hierarchical graph pooling to abstract brain images into a graph structure. Graph Convolutional Networks are then used to learn node embeddings derived from sparse feature vectors. The model attains an accuracy of 87% on the 10-fold cross-validation dataset. This study proves to be cost-effective and efficient in identifying Autism through fMRI, making it suitable for near real-time applications.

**Keywords:** Deep Learning; Machine Learning; Autism Spectrum Disorder; Speech Recognition; Fusion Processing; Information Fusion; Neural networks; Convolutional Neural Network; functional Magnetic Resonance Imaging (fMRI); Autism Brain Imaging Data Exchange (ABIDE)

## 1. Introduction

Per the World Health Organization (WHO) [1], the prevalence of Autism stands at 1 in 100 children, with a noticeable increase in recent times. Autism manifests as a diverse set of conditions impacting brain development. Despite the potential for early detection, Autism is often diagnosed at later stages. The current diagnostic approach for Autism Spectrum Disorder (ASD) relies on interviews, where doctors assess a child's history and behavior, introducing subjectivity. The treatment for Autism is expensive, and there is a shortage of healthcare professionals, especially in developing countries. In recent years, significant progress has been achieved using Artificial Intelligence for Autism detection. Functional Magnetic Resonance Imaging (fMRI) emerges as a non-invasive and cost-effective method for identifying individuals with ASD.

Functional Magnetic Resonance Imaging (fMRI) has been employed to glean physiological insights from active brain regions. Despite the numerous advantages associated with MRI, clinicians often expend significant time to accurately interpret and diagnose individuals with Autism. This extended process may occasionally result in incorrect diagnoses. Compounding the issue, the interpretation of MRI data can pose challenges, particularly as many physicians lack the experience needed to accurately analyze MRI images, making the early-stage diagnosis of Autism Spectrum Disorder (ASD) difficult. Examining the blood oxygenation level dependent signals (BOLD) in brain states unveils irregularities associated with Autism Spectrum Disorder (ASD) [3].

## 2. Related Work

Numerous research endeavors have focused on predicting Autism Spectrum Disorder (ASD) using Machine Learning and Deep Learning algorithms; however, there is a notable scarcity of studies exploring the relationship between autism and brain activity. In a specific study [4], researchers discovered a 1-2% enlargement in the left anterior superior temporal gyrus, brain volume, and grey matter volume in autistic children through an analysis conducted using voxel-based morphometry. Another investigation [5] utilized whole-brain data from fMRI for prediction purposes. In this study, data from 964 subjects across 16 different sites underwent preprocessing to obtain mean BOLD signals for each subject. Pearson correlation coefficient was employed to establish a 7266 x 7266 association matrix representing functional connectivity between Regions of Interest (ROI) pairs. These connections were categorized into bins and subsequently fitted into a linear classifier model. However, the whole-brain classification achieved only a 60% accuracy.

In the study documented in [6], researchers employed a deep learning algorithm by integrating a multi-layer perceptron with autoencoders, achieving a 70% accuracy using the Craddock 200 (CC200) brain atlas. However, the training process was time-consuming, requiring approximately 32 hours. Another approach presented in [7] proposes a framework for ASD detection solely utilizing fMRI data. This method incorporates a joint learning procedure with autoencoders and a single-layered perceptron. Data augmentation involving linear interpolation was applied to the dataset to augment the number of training subjects, resulting in an accuracy of 70.1%. In a separate study [8], researchers achieved a 74% accuracy utilizing a 3D Resnet and MLP classifier.

In this present study, we focus on forecasting ASD versus non-ASD cases, employing deep learning techniques that leverage the temporal dynamic features of BOLD fMRI signals. The emphasis of the study lies in assessing the reliability and reproducibility of outcomes, with potential applications in real-time ASD prediction. Our model outperforms the previous research with temporal dynamic features of BOLD fMRI signals with an accuracy of 87% to detect ASD vs non-ASD.

## 3. Data Analysis

The present study utilizes the Autism Brain Imaging Data Exchange (ABIDE) dataset [8], which includes both fMRI and MRI data. This dataset encompasses 1,112 scanned images, featuring 539 individuals with Autism Spectrum Disorder (ASD) and 573 control individuals. The data is sourced from 17 distinct brain imaging centers.

The techniques described in [9, 10] have been applied in the pre-processing of fMRI signals. We utilized data pre-processed by the Configurable Pipeline for the Analysis of Connectomes (CPAC), involving procedures such as motion correction, slicing, skull stripping, global mean intensity normalization, and nuisance signal regression. Additionally, band-pass filtering and global signal regression were implemented on the dataset as part of the pre-processing steps. It's worth noting that certain features in the dataset exhibit an imbalance, particularly with regard to gender, which serves as a significant factor in predicting Autism Spectrum Disorder (ASD) and influences the accuracy of the predictions. The distribution of Autism and Control individuals by age across various research sites is illustrated in Figure 1.

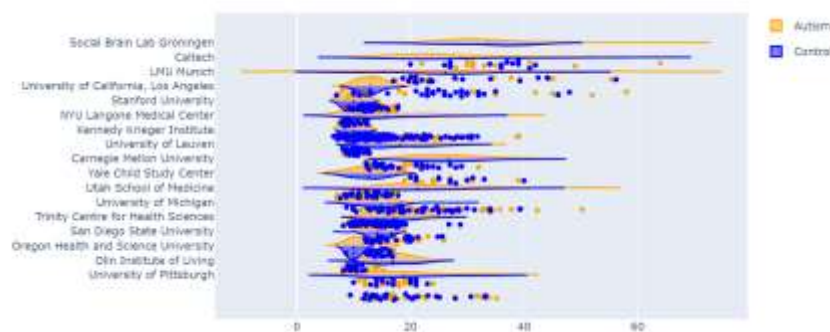


Figure 1: Data Analysis and Preprocessing

To decrease the data dimensionality, the fMRI data is partitioned into signals corresponding to regions of interest (ROIs), which are essentially voxel-wise time series. These ROIs encompass 110 functional brain regions, resulting in the down sampling of the original 4D brain imaging to a 2D data structure,

featuring 110 regions and their respective time series for each area. The Feature Processing pipeline is depicted in Figure 2.

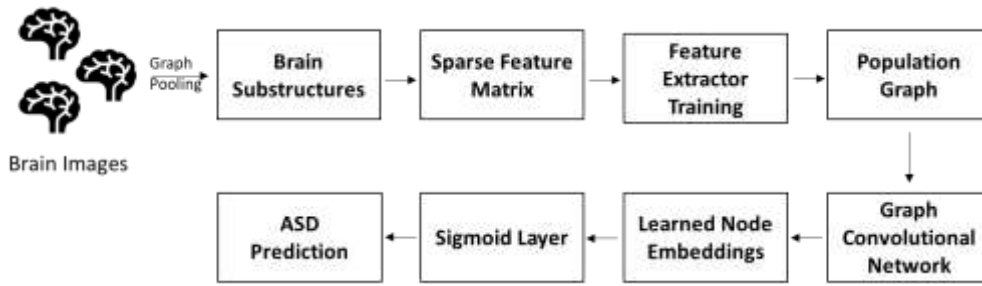


Figure 2: Model Framework

#### 4. Proposed Methodology

Sparse brain networking is achieved through the down sampling of the brain's graph representation utilizing unsupervised graph pooling. Extracting higher-order features is then performed based on the pooling outcomes using a multilayer perceptron. Ultimately, a two-layer graph convolutional network is employed to acquire embeddings through the combination of population graph and phenotypic information.

##### A. Node Selection

Self-attention graph pooling consists of two parts, first it selects the nodes based on the criterion of minimizing the graph information loss and then connect the isolated subgraph caused by the node selection. Unsupervised edge prediction method is used between the two-hop neighbours of each node and itself. Below formula (1) depicts the L1 norm of the Manhattan distance between the node features and one constructed from neighbours.

$$S = \gamma(g) = \|(I - (D^l)^{-1} A^l) H^l\|_1 \quad (1)$$

where  $A^l$  and  $H^l$  are the adjacency and node features matrices of the  $l$ -th layer.  $I$  represent the identity matrix and  $D^l$  denotes the  $l$ -th layer diagonal degree matrix of  $A(l)$ .  $\|\cdot\|$  performs the L1 norm row-wisely. The vector  $S$  contains the information score of each node.

##### B. Edge Prediction

Edge Prediction is a task in graph and network analysis where the goal is to predict missing or future connections between nodes in a network. The goal of edge prediction is to infer which links are most likely to be added or missing based on the observed connections and the structure of the network. We propose a differentiable edge prediction method based on the node features with the help of a self-attention approach to predict underlying links among selected nodes (2).

$$E^l(p, q) = \frac{H^l(p,:) \cdot H^l(q,:)}{\|H^l(p,:)\| \|H^l(q,:)\|} + A^l(p, q) \quad (2)$$

where  $E^l(p, q)$  represents the similarity score between the two nodes,  $H^l$  denotes the feature matrix at the  $l$ -th layer. The corresponding element of adjacency matrix  $A^l(p, q)$  is added to the cosine similarity of the two feature vectors to assign a more significant similarity score to the directly connected nodes.

##### C. Graph Convolutional Networks

GCN is an approach for semi-supervised learning on graph-structured data. In current study, we have used two layers of GCN's namely basic GCN block followed by a clustered Cluster-GCN. GCNs have achieved good performance on arbitrarily structured graphs. Core task is to learn a non-linear function  $f(H^l, A)$  which aggregates the feature vectors of connected nodes to generate features for next layer (3).

$$H^{l+1} = f(H^l, A) = \sigma(\tilde{D}^{-\frac{1}{2}} \tilde{A} \tilde{D}^{-\frac{1}{2}} H^l W^l) \quad (3)$$

with  $\tilde{A} = A + I$ , where  $I$  is the identity matrix and  $\tilde{D}$  is the diagonal node degree matrix of  $\tilde{A}$ . For the  $l$ -th layer of the GCN, the graph can be represented as the feature matrix  $H^l H^0 = X$  and  $H^l = Z$  denote the input and final output feature matrix respectively.  $W^l$  is the learnable weight matrix and  $\sigma(\cdot)$  is the non-linear activation function, ReLU.

In the process of graph pooling, significant subgraphs within the brain network are selected through an unsupervised graph pooling strategy. Graph pooling serves as a down sampling technique crucial in Graph Convolutional Networks for tasks involving graph classification. Prior to graph pooling, either a Multi-Layered Perceptron or a feature-extracting framework from functional connections is constructed. Consequently, the utilization of both functional connections and regional activities demonstrates the superiority of graph pooling in Autism Spectrum Disorder (ASD) detection. The sparse feature details are illustrated in Figure 3.

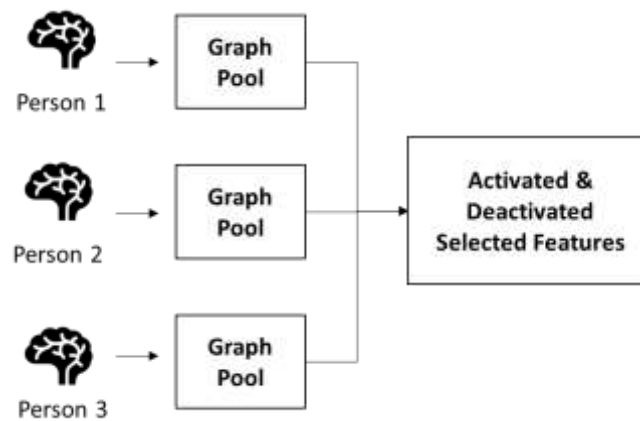


Figure 3: Sparse Feature Details

A population graph is formulated, where edges denote the degree of similarity in phenotypic information, and nodes represent individual subjects. Nodes sharing similar phenotypic information are grouped within the same community. The processing of brain imaging feature vectors is carried out using Graph Convolutional Network (GCN), enabling the learning of node embeddings and extending the convolution operation. Phenotypic information contributes to the regularization of classification performance. The data undergoes preprocessing with CPAC, and the connections between nodes are determined based on phenotypic similarities such as age and gender. The GCN consists of two layers, with the first layer adhering to a conventional GCN framework, and the second layer adopting Cluster-GCN. Visual representations of fMRI images with Regions of Interest (ROI) and images of ROIs post-masking are depicted in Figures 4 and 5, respectively.

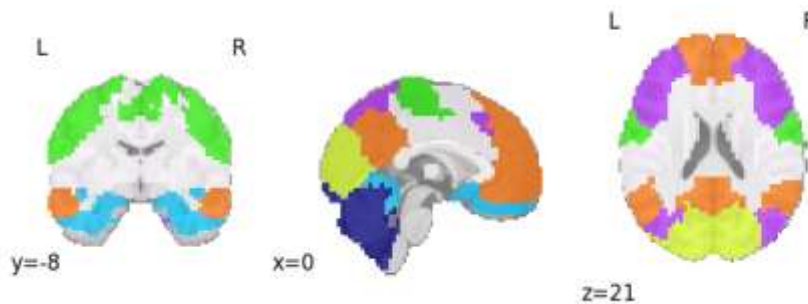


Figure 4: fMRI Images with Region of Interest (ROI)

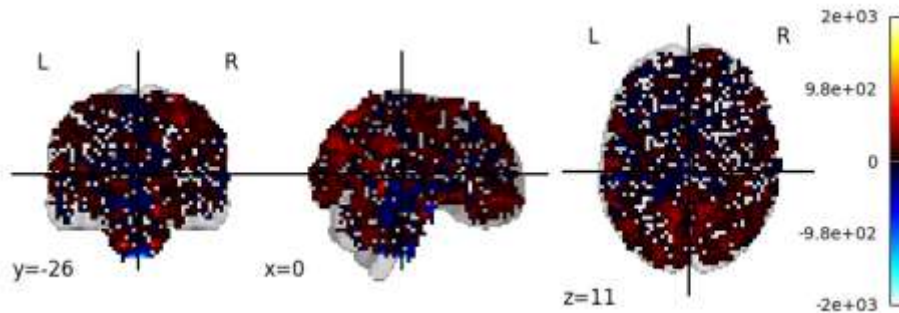


Figure 5: fMRI Images with Region of Interest (ROI) after Masking

Model is evaluated with classification metrics. Below formula is used to calculate Precision(4) and Recall(5) for evaluating the model.

$$\text{Precision} = TP / (TP + FN) \quad (4)$$

$$\text{Recall} = TN / (TN + FP) \quad (5)$$

Where TP: True Positive, TN: True Negative, FP: False Positive, FN: False Negative.

## 5. Results and Discussions

Experiments are conducted using Google Colab due to its GPU requirement. A 10-fold cross-validation process is iterated ten times across the 871 samples. The training of the Graph Convolutional Network and the multilayer perceptron is carried out independently on the same training data. During the multilayer perceptron training, a nested 10-fold cross-validation is implemented, repeating the inner loop five times. Optimization utilizes the Adam optimizer with a learning rate of 0.0001, weight decay of 0.01, and a dropout of 0.01 for GCN generalization. Figure 6 illustrates the Learned Features and Node Embeddings for Gender.

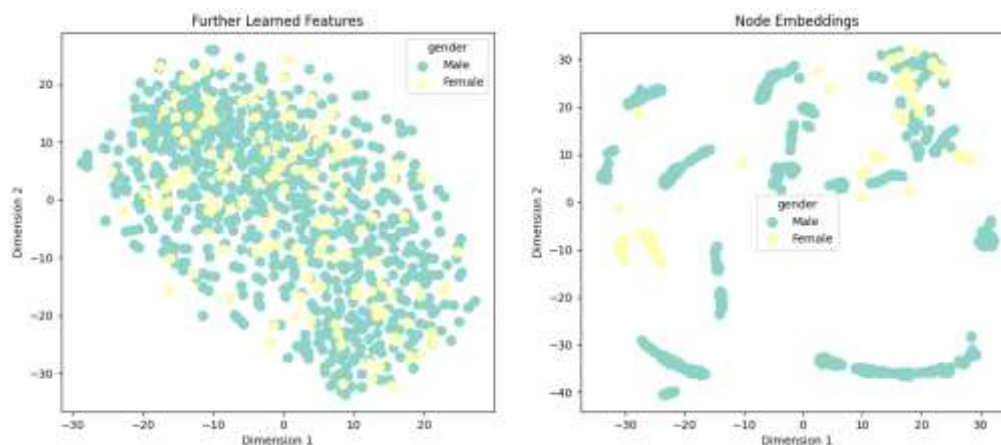


Figure 6: Extracted Features and Embeddings

The ABIDE 1 dataset undergoes preprocessing using CPAC, which employs both single-stage and multi-stage processing. The single stage employs a CNN technique for ASD vs. Control binary classification, yet it yields less satisfactory results due to a scarcity of training samples. The multi-stage approach consists of two components: feature extraction and classification. Feature extractors are trained to extract features from brain functional connections, and a classifier aids in down sampling the brain imaging data. Graph pooling is utilized for this down sampling, and a multilayer perceptron is trained to extract features. The efficiency of graph pooling is assessed with varying pooling ratios.

The model achieves an accuracy of 87%, and recall of 86% surpassing the outcomes of prior studies and demonstrating enhanced robustness in terms of accuracy, specificity, sensitivity, and AUC. The

performance of GCN is notably stable, making it suitable for real-time applications in ASD detection. Figure 7 illustrates the ROC Curve.

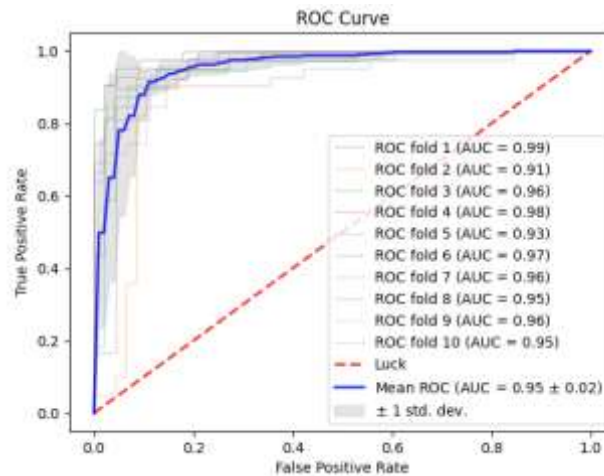


Figure 7: ROC Curve

## 6. Conclusion

Detecting autism at an early stage is a crucial step to mitigate potential complications. This research demonstrates the efficacy of utilizing Artificial Intelligence for autism detection from fMRI data. Employing a down sampling technique for fMRI followed by a graph pooling strategy for feature extraction proved instrumental in comprehending individual variations in brain function. The Graph Convolutional Networks achieved an impressive accuracy of 87% on the ABIDE 1 dataset, showcasing the efficiency of early autism detection. Future investigations will focus on incorporating additional datasets to optimize the model, as well as exploring a multimodal approach by integrating facial and vocal features for enhanced accuracy in autism spectrum disorder (ASD) detection.

## References

- [1] W. H. O., "From: <https://www.who.int/news-room/fact-sheets/detail/autism-spectrum-disorders>", 2023.
- [2] Lord, C.; Rutter, M.; Goode, S.; Heemsbergen, J.; Jordan, H.; Mawhood, L.; Schopler, E. Autism diagnostic observation schedule: A standardized observation of communicative and social behavior. *J. Autism Dev. Disord.* 1989, 19, 185–212.
- [3] Lord, C.; Rutter, M.; Goode, S.; Heemsbergen, J.; Jordan, H.; Mawhood, L.; Schopler, E. Autism diagnostic observation schedule: A standardized observation of communicative and social behavior. *J. Autism Dev. Disord.* 1989, 19, 185–212.
- [4] Riddle, K.; Cascio, C.; Woodward, N. Brain structure in autism: A voxel-based morphometry analysis of the autism brain imaging database exchange (ABIDE). *Brain Imaging Behav.* 2016, 11, 541–551.
- [5] Nielsen, J.; Zielinski, B.; Fletcher, P.; Alexander, A.; Lange, N.; Bigler, E.; Lainhart, J.; Anderson, J. Multisite functional connectivity MRI classification of autism: ABIDE results. *Front. Hum. Neurosci.* 2013, 7, 599.
- [6] Heinsfeld, A.; Franco, A.; Craddock, R.; Buchweitz, A.; Meneguzzi, F. Identification of autism spectrum disorder using deep learning and the ABIDE dataset. *NeuroImage Clin.* 2018, 17, 16–23.
- [7] Eslami, T.; Mirjalili, V.; Fong, A.; Laird, A.; Saeed, F. ASD-DiagNet: A Hybrid Learning Approach for Detection of Autism Spectrum Disorder Using fMRI Data. *Front. Neuroinform.* 2019, 13, 70.
- [8] [Online]. Available: <http://fcon1000.projects.nitrc.org/indi/abide/> (accessed on 23 February 2023).
- [9] C. Craddock, Y. Benhajali, C. Chu, F. Chouinard, A. Evans, A. Jakab, B. S. Khundrakpam, J. D. Lewis, Q. Li, M. Milham et al., "The neuro bureau preprocessing initiative: open sharing of preprocessed neuroimaging data and derivatives," *Frontiers in Neuroinformatics*, vol. 7, 2013.

- [10] Pan, Li et al. "Identifying Autism Spectrum Disorder Based on Individual-Aware Down-Sampling and Multi-Modal Learning." ArXiv abs/2109.09129 (2021): n. pag.
- [11] M. J. Maenner, K. A. Shaw, J. Baio et al., "Prevalence of autism spectrum disorder among children aged 8 years—autism and developmental disabilities monitoring network, 11 sites, united states, 2016," *MMWR Surveillance Summaries*, vol. 69, no. 4, p. 1, 2020.
- [12] L. Crane, J. W. Chester, L. Goddard, L. A. Henry, and E. Hill, "Experiences of autism diagnosis: A survey of over 1000 parents in the united kingdom," *Autism*, vol. 20, no. 2, pp. 153–162, 2016.
- [13] D. P. Carmody and M. Lewis, "Regional white matter development in children with autism spectrum disorders," *Developmental psychobiology*, vol. 52, no. 8, pp. 755–763, 2010.
- [14] M. E. Villalobos, A. Mizuno, B. C. Dahl, N. Kemmotsu, and R.-A. Müller, "Reduced functional connectivity between v1 and inferior frontal cortex associated with visuomotor performance in autism," *Neuroimage*, vol. 25, no. 3, pp. 916–925, 2005.
- [15] N. C. Dvornek, P. Ventola, K. A. Pelphrey, and J. S. Duncan, "Identifying autism from resting-state fmri using long short-term memory networks," in *International Workshop on Machine Learning in Medical Imaging*. Springer, 2017, pp. 362–370.
- [16] A. S. Heinsfeld, A. R. Franco, R. C. Craddock, A. Buchweitz, and F. Meneguzzi, "Identification of autism spectrum disorder using deep learning and the abide dataset," *NeuroImage: Clinical*, vol. 17, pp. 16–23, 2018.
- [17] Z. Sherkatghanad, M. Akhondzadeh, S. Salari, M. Zomorodi-Moghadam, M. Abdar, U. R. Acharya, R. Khosrowabadi, and V. Salari, "Automated detection of autism spectrum disorder using a convolutional neural network," *Frontiers in neuroscience*, vol. 13, p. 1325, 2020.
- [18] M. Khosla, K. Jamison, A. Kuceyeski, and M. R. Sabuncu, "3d convolutional neural networks for classification of functional connectomes," in *Deep Learning in Medical Image Analysis and Multimodal Learning for Clinical Decision Support*. Springer, 2018, pp. 137–145.
- [19] S. Parisot, S. I. Ktena, E. Ferrante, M. Lee, R. Guerrero, B. Glocker, and D. Rueckert, "Disease prediction using graph convolutional networks: application to autism spectrum disorder and alzheimer's disease," *Medical image analysis*, vol. 48, pp. 117–130, 2018.
- [20] J. A. Nielsen, B. A. Zielinski, P. T. Fletcher, A. L. Alexander, N. Lange, E. D. Bigler, J. E. Lainhart, and J. S. Anderson, "Multisite functional connectivity mri classification of autism: Abide results," *Frontiers in human neuroscience*, vol. 7, p. 599, 2013.
- [21] A. Abraham, M. P. Milham, A. Di Martino, R. C. Craddock, D. Samaras, B. Thirion, and G. Varoquaux, "Deriving reproducible biomarkers from multi-site resting-state data: An autism-based example," *NeuroImage*, vol. 147, pp. 736–745, 2017.
- [22] A. Kazeminejad and R. C. Sotero, "The importance of anti-correlations in graph theory based classification of autism spectrum disorder," *Frontiers in neuroscience*, vol. 14, p. 676, 2020.
- [23] S. Mostafa, L. Tang, and F.-X. Wu, "Diagnosis of autism spectrum disorder based on eigenvalues of brain networks," *IEEE Access*, vol. 7, pp. 128 474–128 486, 2019.
- [24] Y. Wang, J. Wang, F.-X. Wu, R. Hayrat, and J. Liu, "Aimafe: autism spectrum disorder identification with multi-atlas deep feature representation and ensemble learning," *Journal of Neuroscience Methods*, p. 108840, 2020.
- [25] J. Liu, Y. Sheng, W. Lan, R. Guo, Y. Wang, and J. Wang, "Improved asd classification using dynamic functional connectivity and multi-task feature selection," *Pattern Recognition Letters*, vol. 138, pp. 82–87, 2020.
- [26] A. A. Sáenz, M. Septier, P. Van Schuerbeek, S. Baijot, N. Deconinck, P. Defresne, V. Delvenne, G. Passeri, H. Raeymaekers, L. Salvesen et al., "Adhd and asd: distinct brain patterns of inhibition-related activation?" *Translational psychiatry*, vol. 10, no. 1, pp. 1–10, 2020.
- [27] G. J. Harris, C. F. Chabris, J. Clark, T. Urban, I. Aharon, S. Steele, L. McGrath, K. Condouris, and H. TagerFlusberg, "Brain activation during semantic processing in autism spectrum disorders via functional magnetic resonance imaging," *Brain and cognition*, vol. 61, no. 1, pp. 54–68, 2006.
- [28] N. Hadjikhani, R. M. Joseph, J. Snyder, and H. Tager-Flusberg, "Abnormal activation of the social brain during face perception in autism," *Human brain mapping*, vol. 28, no. 5, pp. 441–449, 2007.
- [29] S.-Y. Kim, U.-S. Choi, S.-Y. Park, S.-H. Oh, H.-W. Yoon, Y.-J. Koh, W.-Y. Im, J.-I. Park, D.-H. Song, K.-A. Cheon et al., "Abnormal activation of the social brain network in children with autism spectrum disorder: an fmri study," *Psychiatry investigation*, vol. 12, no. 1, p. 37, 2015.
- [30] S. I. Ktena, S. Parisot, E. Ferrante, M. Rajchl, M. Lee, B. Glocker, and D. Rueckert, "Metric learning with spectral graph convolutions on brain connectivity networks," *NeuroImage*, vol. 169, pp. 431–442, 2018.
- [31] Belhaouari SB, Talbi A, Hassan S, Al-Thani D, Qaraqe M. PFT: A Novel Time-Frequency Decomposition of BOLD fMRI Signals for Autism Spectrum Disorder Detection. *Sustainability*. 2023; 15(5):4094. <https://doi.org/10.3390/su15054094>.

- [32] Xin Deng, Jiahao Zhang, Rui Liu, Ke Liu, Classifying ASD based on time-series fMRI using spatial-temporal transformer, *Computers in Biology and Medicine*, Volume 151, Part B, 2022, 106320, ISSN 0010-4825, <https://doi.org/10.1016/j.combiomed.2022.106320>. (<https://www.sciencedirect.com/science/article/pii/S0010482522010289>).
- [33] Khiani, S.; Mohamed Iqbal, M.; Dhakne, A.; Sai Thrinath, B.; Gayathri, P.; Thiagarajan, R. An effectual IOT coupled EEG analysing model for continuous patient monitoring. *Meas. Sens.* 2022, 24, 100597.